Backpropagated Neighborhood Aggregation
for Accurate Training of Spiking Neural Networks

Yukun Yang [1]   **Wenrui Zhang** [1]   **Peng Li** [1]

Abstract

While backpropagation (BP) has been applied to spiking neural networks (SNNs) achieving encouraging results, a key challenge involved is to backpropagate a continuous-valued loss over layers of spiking neurons exhibiting discontinuous all-or-none firing activities. Existing methods deal with this difficulty by introducing compromises that come with their own limitations, leading to potential performance degradation. We propose a novel BP-like method, called neighborhood aggregation (NA), which computes accurate error gradients guiding weight updates that may lead to discontinuous modifications of firing activities. NA achieves this goal by aggregating finite differences of the loss over multiple perturbed membrane potential waveforms in the neighborhood of the present membrane potential of each neuron while utilizing a new membrane potential distance function. Our experiments show that the proposed NA algorithm delivers the state-of-the-art performance for SNN training on several datasets.

1. Introduction

Artificial neural networks (ANNs) have achieved great progress on various tasks including computer vision (Krizhevsky et al., 2017), neural language processing (Brown et al., 2020), reinforcement learning (Berner et al., 2019; Ye et al., 2020), and other big data applications (Niu et al., 2020). Compared with the more conventional non-spiking ANNs, simply referred to as ANNs in this paper, spiking neural networks (SNNs) can exploit efficient temporal codes, exhibit a greater level of biologically plausibility, and achieve significantly improved energy efficiency on neuromorphic hardware (Merolla et al., 2014; Furber

et al., 2014; Davies et al., 2018). While recent SNN research advances have led to improved performance (Zenke & Ganguli, 2018; Shrestha & Orchard, 2018; Wu et al., 2018; Jin et al., 2018; Zhang & Li, 2020; Kim et al., 2020) particularly for tasks that are well suited for SNNs (Blouw et al., 2019; Deng et al., 2020), SNN training is still a challenging task in general.

Backpropagation (BP) has been widely used for training ANNs. Recent works have also demonstrated the great potential of BP in training SNNs (Huh & Sejnowski, 2017; Bellec et al., 2018; Zenke & Ganguli, 2018; Shrestha & Orchard, 2018; Wu et al., 2018; Jin et al., 2018; Wu et al., 2019; Zhang & Li, 2020; Kim et al., 2020; Yang, 2020). Nevertheless, BP based training is complicated by issues such as spatiotemproal dynamics and discontinuities of firing activities in SNNs. Among these, one key challenge is to deal with non-differentiability of firing activities.

To address this difficulty, two main families of BP methods, activation-based (or surrogate gradient) and timing-based methods, and their combination have been proposed (Kim et al., 2020). The activation-based methods approximate the non-differentiable spiking neural activation function by substituting it with a smoothed model (Zenke & Ganguli, 2018; Shrestha & Orchard, 2018; Wu et al., 2018; 2019), allowing error backpropagation in the manner of backpropagation through time (BPTT) or its variants. However, smoothing the non-differentiable activation function effectively converts one actual spike to multiple fictitious spikes and blurs timing information (Zhang & Li, 2020), making learning with precise timing difficult.

On the other hand, timing-based methods train SNNs that code information using spike timing (Bohte et al., 2002; Mostafa, 2017; Zhang & Li, 2020) and are able to accurately compute the gradient of the loss with respect to firing times. Early timing-based methods (Bohte et al., 2002; Mostafa, 2017) are limited to SNNs in which each neuron only fires once. The recent development in this family (Zhang & Li, 2020) can handle more general SNNs where neurons are allowed to fire multiple times, achieving the state-of-the-art results on several datasets including CIFAR-10. The error gradient computed by the timing-based methods is based on a key assumption: the firing count of each neuron remains

unchanged during the training process. In practice this does not prevent adding (removing) spikes to (from) the network during training as demonstrated in (Zhang & Li, 2020), it may cause degradation of weight update precision when the firing counts vary. Moreover, additional tricks such as a warm-up process may be required to bring up the firing activity level of the network before a timing-based method can be applied (Zhang & Li, 2020). Ideas for combining the activation and timing-based methods have been suggested in (Kim et al., 2020).

We propose a new BP method called *neighborhood aggregation* (NA) which acts as a general SNN training method while addressing the limitations of prior activation-based and timing-based methods. The all-or-none nature of spiking activities leads to the non-differentiability of the spiking activation function at firing threshold ϑ, which causes the following fundamental problem. Introducing discrete jumps in the firing activities of an SNN by way of training is essential for achieving a given learning target, e.g., measured by the minimization of a spike-based loss function. However, the conventional error gradient computed by gradient-based training methods corresponds to an infinitesimal change in the loss with respect to the tunable parameters (weights). As such, it cannot accurately guide the introduction of essential discrete jumps in spiking activities nor reliability predict the impact of these jumps on the loss. For activation-based BP methods, this problem surfaces when these methods attempt to compute the derivative of the activation function that does not always exist. Furthermore, spiking models are commonly emulated in discrete time with a finite time step size. Under this case, an infinitesimal change of the membrane potential u that does not move u across the firing threshold at any time, e.g., due to an infinitesimal weight update during training, yields no change in the spike train of the neuron, hence having no impact on the training loss. This implies that: **1)** in order to reduce the training loss, the weight updates must be sufficiently large to alter the spiking activities of the network; and **2)** the surrogate gradient around ϑ computed in the activation-based methods is infinitesimal and does not properly characterize the desired dependency of the loss on the weights.

More generally, we argue that error gradient is not the *best* quantity to look at for training spiking neural networks. As such, in the proposed neighborhood aggregation (NA) method, we resort to finite difference to compute what we refer to as the *aggregated gradient* for characterizing the dependency of the loss on the spiking neural membrane potentials, which also circumvents the difficulty in differentiating the activation function at the firing threshold. The proposed NA is underpinned by three key concepts/components: **1)** the membrane potential neighborhood $\mathbf{N_u} = \{u_p | p = 1, \ldots, M\}$ of a targeted membrane potential waveform u and the construction of $\mathbf{N_u}$, **2)** a

membrane potential distance function (MP-dist), and **3)** a computationally-efficient backpropagated neighborhood aggregation pipeline that outputs the desired aggregated gradient that can be employed to update the weights. Conceptually, $\mathbf{N_u}$ consists of membrane potential waveforms u_p that are close to u and correspond to different spike trains. Hence, $\mathbf{N_u}$ represents likely changes in the membrane potential waveforms introduced by one-step of weight update during training. We compute the dependency of the loss around the present membrane potential waveform u of each spiking neuron within its neighborhood $\mathbf{N_u}$ by aggregating the finite differences of the loss between u_i (each member of $\mathbf{N_u}$) and u. The finite difference operations rely on the proposed distance measure MP-dist. Finally, NA is facilitated by a computationally efficient backpropagated neighborhood aggregation pipeline that leverages the proposed membrane potential neighborhood concept and MP-dist. This pipeline computes the desired aggregated gradient for weight updates in the manner of standard BP methods.

Compared with the prior activation-based methods (Zenke & Ganguli, 2018; Shrestha & Orchard, 2018; Wu et al., 2018; 2019), the proposed NA method does not attempt to differentiate the non-differentiable spiking activation function; instead it computes the aggregated gradient that is more desirable for SNNs exhibiting all-or-none firing characteristics. As a result, it mitigates the poor timing precision of the activation-based methods (Zhang & Li, 2020; Kim et al., 2020). One the other hand, NA does not rely on the assumption of the existing timing-based methods (Mostafa, 2017; Zhang & Li, 2020) that the firing count of each spiking neuron remains constant during training. Hence, the aggregated gradient computed by NA is able to guide weight updates to not only alter the timing of the spikes but also add/remove spikes to minimize the training loss.

Benchmarked by commonly adopted datasets including MNIST (LeCun, 1998), N-MNIST (Orchard et al., 2015), and CIFAR10 (Krizhevsky et al., 2009), the proposed NA algorithm has been shown to outperform the existing state-of-the-art activation and timing-based BP methods for direct training of spiking neural networks and achieve high-accuracy spike computation with low latency.

2. Background

2.1. The Spiking Neuron Model

The leaky integrate-and-fire (LIF) neuron model (Gerstner & Kistler, 2002), one of the most prevalent choices for describing dynamics of spiking neurons, is adopted in this work. During simulation, we use the fixed-step first-order forward Euler method to discretize continuous membrane voltage updates over a set of discrete time steps. The behav-
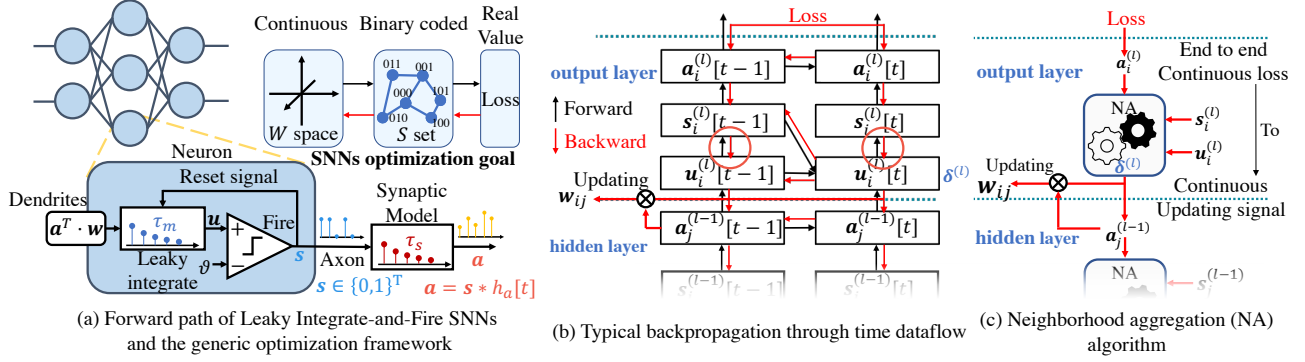
(a) Forward path of Leaky Integrate-and-Fire SNNs and the generic optimization framework

(b) Typical backpropagation through time dataflow

(c) Neighborhood aggregation (NA) algorithm

Figure 1. The forward model of leaky integrate-and-fire SNNs (a), and the backward mechanism comparison between (b) and (c).

ior of a discrete-time LIF neuron can be described by three variables: a, the postsynaptic current (PSC), u, the neuronal membrane potential, and s, the output spike train. All neurons in an SNN share three parameters: τ_m - membrane potential's decaying time constant; τ_s - the time constant of the synaptic function; and ϑ - the firing threshold. The behavior of neuron i in layer l is described by:

$$u_i^{(l)}[t+1] = \left(1 - \frac{1}{\tau_m}\right) u_i^{(l)}[t] \left(1 - s_i^{(l)}[t]\right)$$
$$+ \sum_{j=1}^{N^{(l-1)}} w_{ij}^{(l)} a_j^{(l-1)}[t+1] \tag{1}$$

$$a_i^{(l)} = s_i^{(l)} * \sigma, \quad \sigma[t] = \frac{1}{\tau_s}\left(1 - \frac{1}{\tau_s}\right)^t \tag{2}$$

$$a_i^{(l)}[t+1] = \left(1 - \frac{1}{\tau_s}\right) a_i^{(l)}[t] + \left(\frac{1}{\tau_s}\right) s_i^{(l)}[t+1] \tag{3}$$

$$s_i^{(l)}[t] = H\left(u_i^{(l)}[t] - \vartheta\right) \tag{4}$$

In (1), the $1 - s_i^{(l)}[t]$ term reflects the effect of the firing-and-resetting mechanism and $w_{ij}^{(l)}$ is the weight of the synapse between neuron j in layer $(l-1)$ and neuron i in layer l. The spike train of each presynaptic neuron is processed by a first-order synaptic kernel σ with time constant τ_s (Gerstner & Kistler, 2002) to generate the post-synaptic current (PSC) to the postsynaptic neuron as shown in (2), where (*) represents the time convolution. The same equation can also be written in the form of (3). (4) defines the all-or-none firing activation function for which $H(\cdot)$ represents the Heaviside step function. The synaptic input integration and action potential generation process of an spiking neuron is shown at the bottom of Figure 1 (a), where the neuron is modeled as a nonlinear time-invariant system.

2.2. The Loss Function for Supervised Training

We use the Van Rossum distance (Rossum, 2001) with the same kernel σ used in (2) to measure the difference between the desired output spike-train d and the actual output spike-train s of each output neuron. We denote the loss function

by $L = \sum_{t=0}^{N_t} E[t]$, where N_t is the number of time steps and $E[t]$ is the loss at t. Specifically, L is given by:

$$L = \sum_{t=0}^{N_t} E[t] = \sum_{t=0}^{N_t} \frac{1}{2}\left((\sigma * d)[t] - (\sigma * s)[t]\right)^2$$
$$= \sum_{t=0}^{N_t} \frac{1}{2}\left((\sigma * d)[t] - a[t]\right)^2 \tag{5}$$

Other differentiable loss functions are also usable.

2.3. Backpropagation Flow

Figure 1 (b) shows the spatiotemporal dependencies which shall be considered while training an SNN using a method such as backpropagation through time (BPTT) (Shrestha & Orchard, 2018; Zhang & Li, 2020), where the loss is defined based upon the postsynaptic currents (PSCs) of the output neurons since the same synaptic function kernel is used to define the Van Rossum distance as mentioned before.

Output layer. Without loss of generality we differentiate the right hand of (5), our chosen loss, with respect to each $a_i^{(l)}[t]$ and denote the resulting derivative by $g_i^{(l)}[t]$:

$$g_i^{(l)}[t] = a_i^{(l)}[t] - (\sigma * d_i)[t] \tag{6}$$

Taking into account the temporal dependency in (3), we define $e_i^{(l)}[t] = \frac{\partial L}{\partial a_i^{(l)}[t]}$, which is called a PSC error signal:

$$e_i^{(l)}[t] = \begin{cases} g_i^{(l)}[t], & t = N_t \\ g_i^{(l)}[t] + \frac{\partial a_i^{(l)}[t+1]}{\partial a_i^{(l)}[t]} e_i^{(l)}[t+1], & t < N_t \end{cases} \tag{7}$$

where $\frac{\partial a_i^{(l)}[t+1]}{\partial a_i^{(l)}[t]} = \left(1 - \frac{1}{\tau_s}\right)$ according to (3).

We define $\delta_i^{(l)}[t] = \frac{\partial L}{\partial u_i^{(l)}[t]}$, denoting the backpropagated error for neuron i's membrane potential at time t:

$$\delta_i^{(l)}[t] = \begin{cases} e_i^{(l)}[t] \frac{\partial a_i^{(l)}[t]}{\partial u_i^{(l)}[t]}, & t = N_t \\ e_i^{(l)}[t] \frac{\partial a_i^{(l)}[t]}{\partial u_i^{(l)}[t]} + \delta_i^{(l)}[t+1] \frac{\partial u_i^{(l)}[t+1]}{\partial u_i^{(l)}[t]}, & t < N_t \end{cases} \tag{8}$$

Hidden layers. If layer $(l-1)$ is a hidden layer, $\boldsymbol{g}_i^{(l-1)}[t]$ is defined to be the error backpropagated from layer l's membrane potentials to each $\boldsymbol{a}_i^{(l-1)}[t]$ without considering the temporal dependency between $\boldsymbol{a}_i^{(l-1)}[t]$ at different time points per (1):

$$
\begin{aligned}
\boldsymbol{g}_i^{(l-1)}[t] &= \sum_{p=1}^{N^{(l)}} \left(\frac{\partial u_p^{(l)}[t]}{\partial \boldsymbol{a}_i^{(l-1)}[t]} \frac{\partial L}{\partial u_P^{(l)}[t]} \right) \\
&= \sum_{p=1}^{N^{(l)}} w_{pi}^{(l)} \boldsymbol{\delta}_P^{(l)}[t],
\end{aligned}
\tag{9}
$$

where $N^{(l)}$ is the number of neurons in layer l, and $\boldsymbol{\delta}_i^{(l)}[t]$ is obtained from (8). Recursively applying (7), (8) and (9) backpropagates the errors across all hidden layers.

According to (1), the derivative of loss L with respect to the presynaptic weight $w_{ij}^{(l)}$ of neuron i in layer l shall consider the dependence of L on the neuron's membrane potential $\boldsymbol{u}_i^{(l)}[t]$ at all times:

$$
\frac{\partial L}{\partial w_{ij}^{(l)}} = \sum_{t=0}^{N_t} \frac{\partial \boldsymbol{u}_i^{(l)}[t]}{\partial w_{ij}^{(l)}} \boldsymbol{\delta}_i^{(l)}[t] = \sum_{t=0}^{N_t} \boldsymbol{a}_j^{(l-1)}[t] \boldsymbol{\delta}_i^{(l)}[t]
\tag{10}
$$

2.4. Key Challenges in Backpropagation

In (8), important derivatives to be computed are $\frac{\partial \boldsymbol{a}_i^{(l)}[t]}{\partial \boldsymbol{u}_i^{(l)}[t]}$, which is due to the effect of each neuron's membrane potential on its output PSC, and $\frac{\partial \boldsymbol{u}_i^{(l)}[t+1]}{\partial \boldsymbol{u}_i^{(l)}[t]}$, which reflects the temporal evolution of the membrane potential. As shown by the red circles in Figure. 1, they all need to go through the non-differentiable path $\frac{\partial \boldsymbol{s}_i^{(l)}[t]}{\partial \boldsymbol{u}_i^{(l)}[t]}$, representing the key challenges in backpropagation.

To address the above problems, (Shrestha & Orchard, 2018) approximates the non-differentiable spiking activation function by a probability density function of spike state change, and does not consider the temporal dependencies of a membrane potential across multiple time points. (Wu et al., 2018) substitutes the activation function by a continuous function during backpropagation. Furthermore, this work sets $\frac{\partial \boldsymbol{u}_i^{(l)}[t+1]}{\partial \boldsymbol{u}_i^{(l)}[t]} = (1 - \frac{1}{\tau_m})$, omitting the non-differentiable part of the temporal evolution of membrane potentials. Moreover, both of these methods effectively alter the underlying spiking neuron model and firing times. The more recent work of (Zhang & Li, 2020) instead computes the derivative of the PSC w.r.t. the membrane potential via spike timing to avoid the problem of non-differentiability, enabling learning targeted temporal sequences with high timing precision. However, it cannot directly handle increment and decrement of spike counts during training and requires a warm-up pro-

cess prior to the application of the high-precision BP based training (Zhang & Li, 2020).

As shown in Figure 1(c), the proposed NA method addresses the above problems by computing an aggregated gradient for weights updates to adjust both spike timing and spike counts to minimize the training loss. Specifically, NA computes the critical error signals $\boldsymbol{\delta}_i^{(l)}[t]$ more properly than (8) to allow for weight updates per (10).

3. Methods

3.1. Neighborhood Aggregation (NA): Basic Ideas

The key motivations behind the proposed neighborhood aggregation (NA) method are as follows. The conventional error gradient computed by gradient-based training methods corresponds to an infinitesimal change in the loss with respect to the tunable parameters (weights). As such, it cannot accurately guide the introduction of essential discrete jumps in spiking activities nor reliability predict the impact of these jumps on the loss. Furthermore, for SNNs emulated in discrete time, an incremental weight change does not always produce a sufficiently large perturbation to spiking neurons' membrane potential waveforms $\boldsymbol{u} \in \mathbb{R}^{N_t}$ over N_t time points to alter their output spike trains $\boldsymbol{s} \in \{0, 1\}^{N_t}$. If so, the weight update makes no difference to the training loss. On the other hand, a finite difference of the loss with respect to a sufficiently large perturbation on a neuron's membrane potential can be evaluated even with a non-differentiable spiking activation function. When performed properly and efficiently, finite differences offer a better weight updating strategy for modifying firing activities to reduce the loss.

With respect to the present membrane potential waveform $\boldsymbol{u}$ of a spiking neuron, consider a membrane potential waveform $\boldsymbol{u}'$ close to $\boldsymbol{u}$ and but corresponds to a different spike train $\boldsymbol{s}'$. We call $\boldsymbol{u}'$ a *neighbor* of $\boldsymbol{u}$. While it makes sense to examine the variation of loss L between $\boldsymbol{u}$ and $\boldsymbol{u}'$, however, we do this with a key distinction from all previous BP methods: we use a finite difference as opposed to a derivative of L w.r.t. the membrane potential:

$$
f_{d(\boldsymbol{u}, \boldsymbol{u}')} L = \frac{L(\boldsymbol{u}') - L(\boldsymbol{u})}{\mathrm{d}_{\mathrm{MP}}(\boldsymbol{u}, \boldsymbol{u}')},
\tag{11}
$$

where $\mathrm{d}_{\mathrm{MP}}(\cdot, \cdot)$ is the proposed membrane potential distance *MP-dist* discussed later. The finite difference $f_{d(\boldsymbol{u}, \boldsymbol{u}')} L$ is evaluated over two membrane potentials across N_t time points.

There are three key components in the proposed NA algorithm. First, to compute the finite difference of (11) requires a proper distance function between a given pair of two membrane potential waveforms $\boldsymbol{u}$ and $\boldsymbol{u}'$. For this, we propose the membrane potential distance *MP-dist* that assess the difference between $\boldsymbol{u}$ and $\boldsymbol{u}'$ over N_t time points while

(a) Time domain
membrane potential $\boldsymbol{u}$

(b) Consider $\boldsymbol{u}$ as a
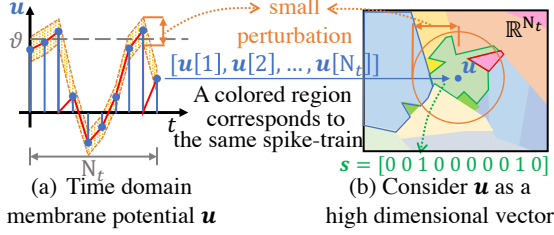high dimensional vector

Figure 2. View membrane potential as a high dimensional vector.

considering the temporal dependency of each membrane potential. Second, we compute $L(\boldsymbol{u}') - L(\boldsymbol{u})$ using a first-order approximation to boost the efficiency of the proposed NA pipeline. Last but not least, a meaningful evaluation of dependency of loss L on the membrane potential via (11) requires proper selection of neighbor $\boldsymbol{u}'$. To do this robustly, we aggregate $f_{d(\boldsymbol{u}, \boldsymbol{u}')} L$ over a set of membrane potentials $\mathbf{N}_{\boldsymbol{u}} = \{\boldsymbol{u}_p | p = 1, \dots, N\}$ that are close to $\boldsymbol{u}$ and correspond to different spike trains. We call this set the *membrane potential neighborhood* of $\boldsymbol{u}$ and discuss ways to construct it. For each $\boldsymbol{u}$, this aggregation leads to a vector $\widetilde{\nabla}_{\boldsymbol{u}} L$ defined over N_t time points and called the *aggregated gradient*. Ultimately, $\widetilde{\nabla}_{\boldsymbol{u}} L$ replaces the error vector $\boldsymbol{\delta}_i^{(l)}$ in (10) to perform layer-by-layer backpropagation.

3.2. Membrane Potential Space

We consider the membrane potential $\boldsymbol{u}$ of a neuron as a high dimensional vector in $\mathbb{R}^{N_t}$ as in Figure 2. At each time point, whenever $\boldsymbol{u}[t]$ exceeds the firing threshold ($\boldsymbol{u}[t] \geq \vartheta$), a spike is generated. Conversely, whenever $\boldsymbol{u}[t]$ falls within the range of $\boldsymbol{u}[t] < \vartheta$, there is no spike. Therefore, membrane potential waveforms that correspond to the same spike train can be grouped together to form a *region* . All membrane potentials $\boldsymbol{u} \in \mathbb{R}^{N_t}$ are divided into many continuous regions corresponding to different spike trains represented by different colors in Figure 2.

Key neighbors. To compute the finite difference $f_{d(\boldsymbol{u}, \boldsymbol{u}')} L$ of (11), we choose each $\boldsymbol{u}'$ belonging to a region $\boldsymbol{G}'$ different from region $\boldsymbol{G}$ where $\boldsymbol{u}$ is. This is to consider adding perturbations to $\boldsymbol{u}$ to create a change in the spike train. While sharing the same spike train $\boldsymbol{s}'$, membrane potential waveforms in $\boldsymbol{G}'$ have a different distance to $\boldsymbol{u}$. We call $\boldsymbol{u}'_k \in \boldsymbol{G}$ that is closest to $\boldsymbol{u}$ a *key neighbor* of region $\boldsymbol{G}'$. Only key neighbors in different regions are chosen to form the membrane potential neighborhood of $\boldsymbol{u}$: $\mathbf{N}_{\boldsymbol{u}} = \{\boldsymbol{u}_p | p = 1, \dots, n\}$. Practical ways for constructing $\mathbf{N}_{\boldsymbol{u}}$ is discussed in Section 3.4.

3.3. Membrane Potential Operations and Distance

While distance concepts have been discussed for binary spike trains (Victor & Purpura, 1997), a distance function is needed to quantify the difference between a pair of two continuous-valued membrane potential waveforms $\boldsymbol{u}$ and $\boldsymbol{u}'$ over N_t time points in (11). Modifying the membrane poten-

tial $\boldsymbol{u}[t]$ of a neuron at time t may impact $\boldsymbol{u}[t'], t' \geq t$ due to the dependencies introduced by the temporal evolution of $\boldsymbol{u}$. To this end, the key drawback of applying existing distances for multiple-dimensional vectors such as the Hamming distance is that no temporal relationship among components of a vector is considered.

We propose a novel membrane potential distance *MP-dist* denoted by $\mathrm{d}_{\mathrm{MP}}(\cdot, \cdot)$ to consider temporal dependencies between the values of the membrane potential at different time points. According to the dynamics of LIF neurons in (1), membrane potential $\boldsymbol{u}_i^{(l)}$ of neuron i can be obtained by integrating the total synaptic input $\boldsymbol{c}_i^{(l)} \in \mathbb{R}^{N_T}$, with $\boldsymbol{c}_i^{(l)}[t] = \sum_j w_{ij}^{(l)} \boldsymbol{a}_j^{(l-1)}[t]$, from a known initial condition. For the convenience of discussion, we define the function that maps from a given total synaptic input $\boldsymbol{c}$ to the corresponding membrane potential $\boldsymbol{u}$: $f(\boldsymbol{c}) = \boldsymbol{u}$. This mapping can be simply obtained by computing $\boldsymbol{u}$ using (1) to (4). The inverse of f maps from $\boldsymbol{u}$ to $\boldsymbol{c}$: $f^{-1}(\boldsymbol{u}) = \boldsymbol{c}$. Note that $\boldsymbol{c}$ is readily available in each forward pass during training such that f^{-1} need not be explicitly constructed.

In the N_t-dimensional membrane potential space $\boldsymbol{U} = \mathbb{R}^{N_t}$, we define a commutative binary addition operator $\boxplus : \boldsymbol{U} \times \boldsymbol{U} \to \boldsymbol{U}$, which adds two given membrane potentials (vectors) $\boldsymbol{u}$ and $\boldsymbol{\epsilon}$ to produce a summed membrane potential $\boldsymbol{u}' = \boldsymbol{u} \boxplus \boldsymbol{\epsilon}$ according to Algorithm 1. By making use of $\boxplus$, we can perturb the present membrane potential $\boldsymbol{u}$ by adding a perturbation $\boldsymbol{\epsilon}$ to it. Importantly, $\boxplus$ is not the element-wise addition. Instead, $\boldsymbol{\epsilon}[t]$ is included in the total synaptic input to the neuron at time t during the membrane potential integration process per (1). Hence, $\boldsymbol{\epsilon}[t]$ may impact the resulting membrane potential at both the present and future times, i.e., $\boldsymbol{u}'[t'], t' \geq t$. In other words, $\boldsymbol{\epsilon}$ is added to $\boldsymbol{u}$ while considering the chain effects exerted on future time points. Under the same spirit, we define a binary subtraction operator $\boxminus : \boldsymbol{U} \times \boldsymbol{U} \to \boldsymbol{U}$ as described in Algorithm 2. $\boxminus$ finds the difference between a given pair of two membrane potentials $\boldsymbol{u}$ and $\boldsymbol{u}'$, which is $\boldsymbol{\epsilon} = \boldsymbol{u}' \boxminus \boldsymbol{u}$, such that $\boldsymbol{u}' = \boldsymbol{u} \boxplus (\boldsymbol{u}' \boxminus \boldsymbol{u})$. Essentially, $\boxminus$ subtracts $\boldsymbol{u}$ from $\boldsymbol{u}'$ while considering the chain effects on future time points. It can be shown that $\boldsymbol{u}' \boxminus \boldsymbol{u} = -(\boldsymbol{u} \boxminus \boldsymbol{u}')$.

The proposed membrane potential distance $\mathrm{d}_{\mathrm{MP}}(\cdot, \cdot) : \boldsymbol{U} \times$

Algorithm 1 Membrane potential addition: $\boldsymbol{u}' = \boldsymbol{u} \boxplus \boldsymbol{\epsilon}$

Inputs: $\boldsymbol{u}, \boldsymbol{\epsilon}$;   **Output:** $\boldsymbol{u}'$; ϑ: firing threshold;
Initialization: $u = 0$;
$\boldsymbol{c} = f^{-1}(\boldsymbol{u})$;
for t in $range(1, N_t)$**:**
$\quad \boldsymbol{u}'[t] = u\left(1 - \frac{1}{\tau_m}\right) + \boldsymbol{\epsilon}[t] + \boldsymbol{c}[t]$;
$\quad u = \boldsymbol{u}'[t]\left(1 - H(\boldsymbol{u}'[t] - \vartheta)\right)$;
return $\boldsymbol{u}'$

Algorithm 2 Membrane potential subtraction: $\boldsymbol{\epsilon} = \boldsymbol{u}' \boxminus \boldsymbol{u}$

Inputs: $\boldsymbol{u}, \boldsymbol{u}'$; Output: $\boldsymbol{\epsilon}$; ϑ: firing threshold;
initialization: $u = 0$;
$\boldsymbol{c} = f^{-1}(\boldsymbol{u})$;
for t in $range(1, N_t)$**:**
$\quad \boldsymbol{u}[t] = u(1 - \frac{1}{\tau_m}) + \boldsymbol{c}[t]$;
$\quad \boldsymbol{\epsilon}[t] = \boldsymbol{u}'[t] - \boldsymbol{u}[t]$;
$\quad u = \boldsymbol{u}'[t]\Big(1 - H(\boldsymbol{u}'[t] - \vartheta)\Big)$;
return $\boldsymbol{\epsilon}$

$\boldsymbol{U} \to [0, +\infty)$ is a metric in the membrane potential space $\boldsymbol{U} = \mathbb{R}^{N_t}$ and is defined by $\mathrm{d}_{\mathrm{MP}}(\boldsymbol{u}, \boldsymbol{u}') = \|\boldsymbol{u}' \boxminus \boldsymbol{u}\|_2$. Unitizing $\boxplus$, $\boxminus$, and $\mathrm{d}_{\mathrm{MP}}(\cdot, \cdot)$, one can find key neighbors of the present membrane potential $\boldsymbol{u}$ by adding perturbations to it, form the membrane potential neighborhood $\mathbf{N}_{\boldsymbol{u}}$ of $\boldsymbol{u}$, and determine the distances between $\boldsymbol{u}$ and the members of $\mathbf{N}_{\boldsymbol{u}}$ for computing the finite differences of Loss L.

3.4. Simple Neighborhood Selection (SNS)

To well represent the landscape of the loss in the membrane potential space, for each spiking neuron one may choose n closest neighbors evaluated by $\mathrm{d}_{\mathrm{MP}}(\cdot, \cdot)$ to form a neighborhood $\mathbf{N}_{\boldsymbol{u}}$ of the present membrane potential $\boldsymbol{u}$. However, it is not obvious how to design an algorithm to find the top n nearest key neighbors from a total of 2^{N_t} regions in the membrane potential space with an acceptable computational complexity. As a first step, we propose a simple and effective strategy named SNS (Simple Neighborhood Selection). To select neighbors that are close to $\boldsymbol{u} \in \mathbb{R}^{N_t}$, SNS introduces a set of N_t membrane potential perturbations: $\boldsymbol{\epsilon}_{(i)}, i = 1, \cdots, N_t$, where $\boldsymbol{\epsilon}_{(i)}[j] = 0, \forall j \neq i$ and $\boldsymbol{\epsilon}_{(i)}[i] \neq 0$. With $\boldsymbol{\epsilon}_{(i)}$ only a non-zero perturbation is introduced at time point i. $\boldsymbol{\epsilon}_{(i)}[i]$ is chosen to be the least amount of membrane potential perturbation that can cause a firing

(a) A membrane potential waveform

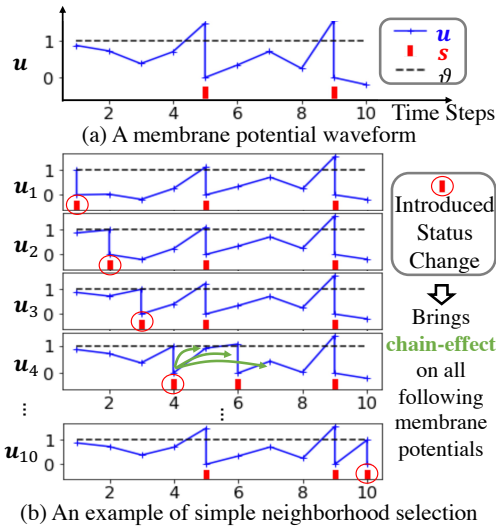(b) An example of simple neighborhood selection

Figure 3. Simple neighborhood selection (SNS).

status change, i.e., firing to no firing or vice versa, at time point i. The initialized firing status change trickles down to later time points, causing additional membrane potential changes. This chain-effect can be captured by Algorithm 1, which effectively produces a perturbed membrane potential $\boldsymbol{u}_{(i)} = \boldsymbol{u} \boxplus \boldsymbol{\epsilon}_{(i)}$. We construct a N_t-member neighborhood $\mathbf{N}_{\boldsymbol{u}} = \{\boldsymbol{u}_{(i)} | i = 1, \ldots, N_t\}$. This process is illustrated in Figure 3 (b). The exploration of other neighborhood selection techniques is left for future work.

3.5. The NA Algorithm Pipeline

Processing of a single network layer l by the NA algorithm consists of five steps. The time argument and neuron and layer indices are dropped to simplify notations when causing no confusion.

Step 1. PSC Error Signal Computation: (6), (7), and (9) are on the differentiable path. Combining (6) and (9) gives:

$$\boldsymbol{g}_i^{(l)} = \begin{cases} \boldsymbol{a}_i^{(l)} - (\boldsymbol{\sigma} * \boldsymbol{d}_i), & \text{output layer} \\ \sum_{p=1}^{N^{(l+1)}} w_{ji}^{(l+1)} \boldsymbol{\delta}_p^{(l+1)}, & \text{hidden layer} \end{cases} \quad (12)$$

Plugging (12) into (7) produces the desired PSC error signal $\boldsymbol{e}_i^{(l)}$ for neuron i, which will used in Step 4.

Step 2. Neighborhood Selection: Following our earlier discussions, for each neuron one may choose M key neighbors of the present membrane potential, corresponding to different spike trains. This can be done by adding perturbations to the membrane potential using SNS.

Step 3. Membrane Potential Distance Computation: The distance between the present membrane potential $\boldsymbol{u}$ of a neuron and each key neighbor $\boldsymbol{u}_p$ in its neighborhood $\mathbf{N}_{\boldsymbol{u}}$ is determined using $\mathrm{d}_{\mathrm{MP}}(\cdot, \cdot)$ through Algorithm 2.

Step 4. First-order Loss Approximation: Per (11), it is necessary to evaluate the loss $L(\boldsymbol{u}_p)$ at each neighbor $\boldsymbol{u}_p$ to compute the variation of the loss, which can be done by performing an additional forward propagation from the current layer to the output layer. Such repeatedly forward propagations for all neurons' neighborhoods add an unacceptable computational overhead to the training process. Noting that $L(\boldsymbol{u}_p) = L(\boldsymbol{a}(\boldsymbol{u}_p)) \equiv L(\boldsymbol{a}_p)$, we address this difficulty by using the PSC error signal $\boldsymbol{e} = \nabla_{\boldsymbol{a}} L$ given by (7) to estimate the variation of the loss due to the perturbation introduced to the PSC $\boldsymbol{a}$. It is important to note that $\boldsymbol{e}$ is readily available in **Step 1**.

As shown in Figure 4, using $\boldsymbol{e} \in \mathbb{R}^{N_t}$ for a first-order approximation means approximating the loss landscape by a tangent hyper-plane around the present PSC $\boldsymbol{a}$. The first-order approximation of the change of the loss between the current PSC $\boldsymbol{a}$ and one of its near neighbor's PSC $\boldsymbol{a}_p$ is:

$$\begin{aligned} L(\boldsymbol{a}_p) - L(\boldsymbol{a}) &\approx \nabla_{\boldsymbol{a}} L(\boldsymbol{a}_p - \boldsymbol{a}) \\ &= \boldsymbol{e} \cdot (\boldsymbol{a}_p - \boldsymbol{a}) \end{aligned} \quad (13)$$
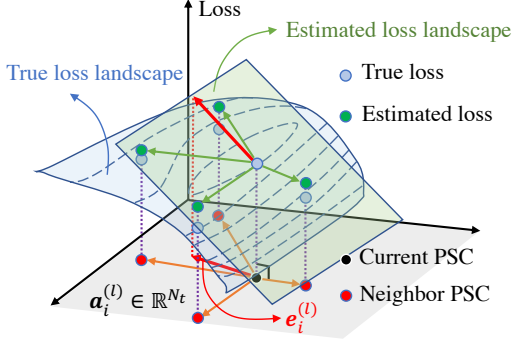
Figure 4. First order loss approximation

As such, NA achieves great computational efficiency via first-order approximations of loss changes without expensive forward propagations.

Step 5. Neighborhood Aggregation and Weight Updates: As discussed earlier in terms of (11), instead of attempting to compute the conventional gradient $\nabla_{\boldsymbol{u}} L \in \mathbb{R}^{N_t}$ which does not exist everywhere for spiking neurons, we compute the finite difference $f_{d(\boldsymbol{u}, \boldsymbol{u}_p)} L$ between $\boldsymbol{u}$ and one of its near neighbor $\boldsymbol{u}_p$ while using (13):

$$f_{d(\boldsymbol{u}, \boldsymbol{u}_p)} L = \frac{L(\boldsymbol{u}_p) - L(\boldsymbol{u})}{d_{\mathrm{MP}}(\boldsymbol{u}, \boldsymbol{u}_p)} \approx \frac{\boldsymbol{e} \cdot (\boldsymbol{a}_p - \boldsymbol{a})}{d_{\mathrm{MP}}(\boldsymbol{u}, \boldsymbol{u}_p)}, \quad (14)$$

which only captures the variation of loss between $\boldsymbol{u}$ and $\boldsymbol{u}_p$. Here we compute an aggregated gradient $\widetilde{\nabla}_{\boldsymbol{u}} L \in \mathbb{R}^{N_t}$ over the neuron's entire M-member neighborhood based on all $f_{d(\boldsymbol{u}, \boldsymbol{u}_p)} L$, where $p = 1, 2, \ldots, M$. For this, we consider each $f_{d(\boldsymbol{u}, \boldsymbol{u}_p)} L$ as the directional derivative resulted from projecting $\widetilde{\nabla}_{\boldsymbol{u}} L$ onto the unit perturbation vector $\boldsymbol{o}_p = \frac{\boldsymbol{u}_p \boxminus \boldsymbol{u}}{||\boldsymbol{u}_p \boxminus \boldsymbol{u}||_2} = \frac{\boldsymbol{u}_p \boxminus \boldsymbol{u}}{d_{\mathrm{MP}}(\boldsymbol{u}, \boldsymbol{u}_p)}$, leading to a system of linear equations on the left of (15):

$$\begin{bmatrix} \boldsymbol{o}_1^T \\ \boldsymbol{o}_2^T \\ \vdots \\ \boldsymbol{o}_M^T \end{bmatrix} \cdot \widetilde{\nabla}_{\boldsymbol{u}} L = \begin{bmatrix} f_{d(\boldsymbol{u}, \boldsymbol{u}_1)} L \\ f_{d(\boldsymbol{u}, \boldsymbol{u}_2)} L \\ \vdots \\ f_{d(\boldsymbol{u}, \boldsymbol{u}_M)} L \end{bmatrix}, \widetilde{\nabla}_{\boldsymbol{u}} L = \begin{bmatrix} \boldsymbol{o}_1^T \\ \boldsymbol{o}_2^T \\ \vdots \\ \boldsymbol{o}_M^T \end{bmatrix}^{+} \begin{bmatrix} f_{d(\boldsymbol{u}, \boldsymbol{u}_1)} L \\ f_{d(\boldsymbol{u}, \boldsymbol{u}_2)} L \\ \vdots \\ f_{d(\boldsymbol{u}, \boldsymbol{u}_M)} L \end{bmatrix}$$

(15)

$\widetilde{\nabla}_{\boldsymbol{u}} L$ is solved according to the right side of (15). $+$ is the Moore–Penrose pseudoinverse considering that the system matrix may not always be invertible.

Using $\widetilde{\nabla}_{\boldsymbol{u}} L$ to substitute $\boldsymbol{\delta}$ in (10) allows for weight updates of layer l, after which the backprogagation proceeds to the preceding layer.

3.5.1. FURTHER SIMPLIFICATIONS UNDER SNS

The simplicity of neighborhood selection using SNS brings additional advantages. First, the MP-dist between $\boldsymbol{u}$ and any of its neighbors $\boldsymbol{u}_p$ in the formed neighborhood is simply: $d_{\mathrm{MP}}(\boldsymbol{u}, \boldsymbol{u}_p) = \vartheta - \boldsymbol{u}[p]$. The M unit perturbation vectors $\{\boldsymbol{o}_1, \boldsymbol{o}_2, \ldots, \boldsymbol{o}_M\}$ in (15), where $M = N_t$, form an identity

matrix. As a result, the right side of (15) reduces to:

$$\widetilde{\nabla}_{\boldsymbol{u}} L = \begin{bmatrix} f_{d(\boldsymbol{u}, \boldsymbol{u}_1)} L \\ f_{d(\boldsymbol{u}, \boldsymbol{u}_2)} L \\ \vdots \\ f_{d(\boldsymbol{u}, \boldsymbol{u}_M)} L \end{bmatrix} \quad (16)$$

Hence, the aggregated gradient $\widetilde{\nabla}_{\boldsymbol{u}} L$ can be efficiently obtained without computing the pseudoinverse in the right side of (15).

4. Experimental Results

We designed several experiments to demonstrate the effectiveness of the proposed membrane potential distance MP-dist and the NA algorithm while comparing with several other SNN training algorithms. Moreover, we provided a time-complexity analysis of several algorithms with a wall-clock time comparison.

4.1. MP-dist Quality Evaluation

The finite difference based aggregated gradient computation highly relies on an accurate measure of distance between a given membrane potential $\boldsymbol{u}$ and its neighbor $\boldsymbol{u}_p$. While inducing discrete jumps in firing activity, small weight updates in training shall modify the present $\boldsymbol{u}$ to a close neighbor $\boldsymbol{u}_p$ that corresponds to a small MP-dist from $\boldsymbol{u}$.

To evaluate the quality of the MP-dist distance $d_{\mathrm{MP}}(\cdot, \cdot)$, we counted the changes of all neurons' spike-trains of the SNN with the same architecture used in Table 2. The SNN was trained by TSSL-BP(Zhang & Li, 2020) on the MNIST dataset (LeCun, 1998) in 100 training iterations with a total number of time-steps $N_T = 10$, as shown in Figure 5 (a). The input samples were kept the same before and after an training iteration to count the spike train changes. The decimal index of a spike train was converted from its corresponding binary code (e.g. $[1, 1, 1, 1, 1, 1, 1, 1, 1, 1] \rightarrow 1023$, $[0, 0, 0, 0, 0, 0, 0, 1, 0, 1] \rightarrow 5$).

Each pixel in Figure 5 (a) represents the count of transfers from a particular spike train (y-index) before a train-

(a) Spike train transfer matrix

(b) MP-dist quality evaluation
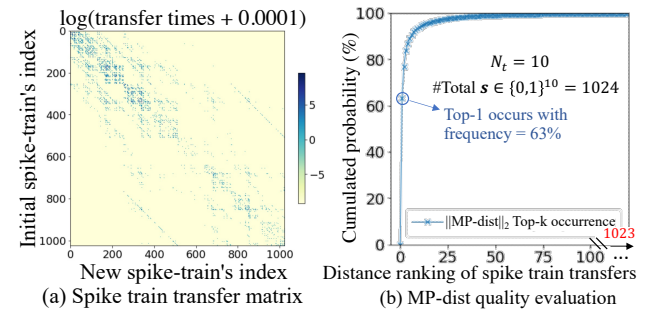
Figure 5. The quality evaluation of MP-dist $d_{\mathrm{MP}}(\cdot, \cdot)$.

ing weight update iteration to another spike train (x-index) after the iteration. We accumulated the counts for all neurons' output spike trains in the 100 iterations. For example, "$(4, 5) = 12$" means that the transition from the output spike train $[0, 0, 0, 0, 0, 0, 0, 1, 0, 0](\rightarrow 4)$ to the output spike train $[0, 0, 0, 0, 0, 0, 0, 1, 0, 1](\rightarrow 5)$ happened 12 times.

The values on the main diagonal of the transfer matrix represent the total number of cases that the corresponding output spike train remained unchanged before and after an training iteration, which are very large and uninformative. For ease of visualization, we set these values to zero and also showed the transfer counts in log scale to make small values visible.

Figure 5 (b) shows the cumulative probability distribution (CDF) of the ranking of the distance between the spike train before a training iteration and the one after the iteration evaluated using $d_{MP}(\cdot, \cdot)$ based on the data tracked over all possible discrete spike train transfers of all neurons. To more meaningfully visualize the CDF, we ranked the collected $d_{MP}(\cdot, \cdot)$, and displayed the ranking in the ascending order along the x-axis of Figure 5 (b). Based on MP-dist, the spike train transfers with the least $d_{MP}(\cdot, \cdot)$ value represent transfers between the closet spike trains or within the top-1 nearest regions in the membrane potential space, which constituted a high percentage (63%) of all transfers observed. The CDF reaches to 100% quickly. This results confirm the quality of MP-dist: a large majority of the neurons' output spike trains indeed changed to a spike train with a small MP-dist value.

4.2. A Single-neuron Network

This subsection demonstrates how the output neuron's spike-train changes towards the desired one in a single-neuron network (Figure 6 (a)) with two different learning algorithms. The parameters used are summarized in Table 1. 500 independent training experiments (rounds), each with a different set of randomly generated spike inputs and desired output spike train, were conducted.

Table 1. Parameters of the single-neuron network.

N_T	#inputs	p_{in}	#iters	#rounds	p_o	τ_s	τ_m
30	200	0.05	200	500	0.2	2	5

In each round, we randomly generated spikes for all 200 input neurons. The activity of the i-th input spike train at time step t, $\boldsymbol{s}_i[t]$, followed the Bernoulli distribution with $p(\boldsymbol{s}_i[t] = 1) = p_{in}$, for $i = 1, 2, ..., 200$. The PSC $\boldsymbol{a}_i$ generated by the i-th input neuron was computed based on a chosen synaptic function kernel $\boldsymbol{\sigma}$ by $\boldsymbol{a}_i = \boldsymbol{s}_i * \boldsymbol{\sigma}$, we use $\boldsymbol{\sigma}$ as in (2), with $\tau_s = 2$. We then normalized using the mean and standard deviation of all PSCs. The input currents are then feed into the single output neuron with its membrane potential time constant $\tau_m = 5$. Similarly, the desired output spike train $\boldsymbol{s}_o$ of the single output neuron, i.e.,

(a) Single-neuron network

(b) Mean and std of all loss curves
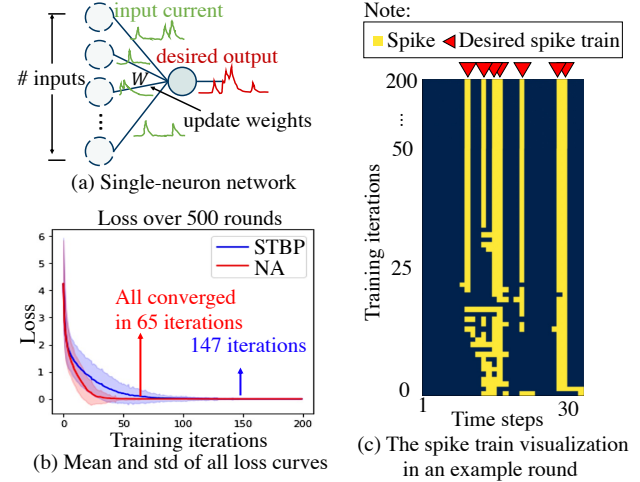
(c) The spike train visualization in an example round

Figure 6. Training of the single-neuron network.

the label, was randomly generated following the Bernoulli distribution with probability $p(\boldsymbol{s}_o[t] = 1) = p_o$. Figure 6 (c) shows an example of how the neuron's output spike train changes towards the desired one with the NA algorithm in a single round.

We compared our NA algorithm with the recent activation-based surrogate gradient method STBP (Wu et al., 2018; 2019) by training the weights between the input neurons and the single output neuron for 200 iterations in each round. The loss function we use here is (5). We recorded the variation of the loss during the 200 iterations, and repeated the same experiment for 500 rounds. The recorded 500 loss curves are shown in Figure 6 (b). The solid lines are the mean values of the 500 loss curves while the shaded areas illustrate the standard deviations. Clearly, the proposed NA algorithm reduced the losses quickly and could converge to the desired output firing patterns within 65 iterations. In contrast, STBP (Wu et al., 2019) did not all converge to the desired output patterns until 147 iterations.

4.3. The Results on the MNIST Dataset

The proposed NA algorithm is compared with with several other SNN BP training methods for training a spiking convolutional neural network (CNN) on the MNIST dataset (LeCun, 1998) in Table 2. The NA algorithm used only

Table 2. Performances of different SNN BP methods on MNIST.

Method	#Steps	BestAcc
HM2BP (Jin et al., 2018)	400	99.49%
ST-RSBP (Zhang & Li, 2019)	400	99.62%
SLAYER (Shrestha & Orchard, 2018)	300	99.41%
STBP (Wu et al., 2018)	30	99.42%
TSSL-BP (Zhang & Li, 2020)	5	99.53%
This work	**5**	**99.69%**

Spiking CNN structure: 15C5-P2-40C5-P2-300

a total of five time steps, same as for TSSL-BP (Zhang & Li, 2020), and gained the best accuracy among all these methods, showing its potential in accurate training of SNNs with short temporal latency.

4.4. The Results on the N-MNIST Dataset

The N-MNIST (Orchard et al., 2015) is the neuromorphic version of the MNIST dataset (LeCun, 1998). We adopted the same spiking CNN structure following TSSL-BP (Zhang & Li, 2020) and SLAYER (Shrestha & Orchard, 2018). Each input example of the original N-MNIST dataset is over 300,000 time steps. We reduced the time resolution to 100 time steps following the procedure described in (Zhang & Li, 2020). STBP (Wu et al., 2019) applied spike accumulation instead, and reduced the time resolution to 300 time steps. To demonstrate the strength of the proposed NA method, we further compressed each input example by retaining only the beginning 30% portion of the input spike trains to train a spiking CNN based on the architecture specified in Table using the NA algorithm over a short time window of 30 time points. And yet, our NA algorithm outperforms all other methods based on the same spiking CNN architecture as reported in Table 3.

Table 3. Performances of different SNN BP methods on N-MNIST.

Methods	#Time steps	Best accuracy
SLAYER	300	99.22%
TSSL-BP	100	99.40%
TSSL-BP	30	99.28%
This work	30	**99.35%**

Spiking CNN structure: 12C5-P2-64C5-P2

4.5. The Results on the CIFAR10 Dataset

The CIFAR10 dataset (Krizhevsky et al., 2009) is a challenging image dataset for testing direct training of SNNs. Table 4 compares the accuracy of SNNs based on the widely adopted Alexnet and CifarNet architectures trained by three different BP methods. Within a short time window of five time steps, the Alexnet model trained by our NA algorithm had the best accuracy, which even surpassed the performance of the larger CifarNet model trained by the STBP algorithm (Wu et al., 2019) over a longer time window.

Table 4. Performances of different SNN BP methods on CIFAR10.

Methods	Structure	#Time steps	Best accuracy
STBP	AlexNet	12	85.24%
STBP	CifarNet	12	90.53%
TSSL-BP	AlexNet	5	89.22%
This work	AlexNet	5	**91.76%**

AlexNet structure: 96C3-256C3-P2-384C3-P2-384C3-256C3-1024-1024
CifarNet structure: 128C3-256C3-P2-512C3-P2-1024C3- 512C3-1024-512

4.6. Time Complexity Analysis

The time complexity of both STBP (Wu et al., 2019) and TSSL-BP is $\mathcal{O}(N_t)$, where N_t is the number of time steps. With neighborhood selection using SNS, NA perturbs the membrane potential of each spiking neuron N_t times and computes the resulting neighbors by running Algorithm 1 N_t times. Since a single run of Algorithm 1 has a complexity of $\mathcal{O}(N_t)$, the overall complexity of NA is $\mathcal{O}(N_t^2)$.

Figure 7 reports the wall-clock times consumed by one training epoch of STBP, TSSL-BP, and NA, respectively, for training the spiking CNNs of Table 2. While having a higher theoretical complexity, NA is faster than TSSL-BP (Zhang & Li, 2020) when $N_t = 5$, which may be due to differences in code optimization. The complexity of NA may be lowered by choosing fewer but more important membrane potential neighbors or limiting the range of temporal dependencies considered in Algorithm 1, which will be explored in our future work.
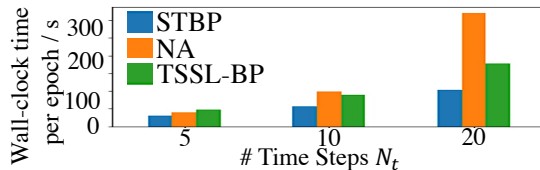

Figure 7. Wall-clock time comparison (MNIST dataset, single TITAN XP GPU, BatchSize=64)

5. Conclusion

We presented a new SNNs direct training method, neighborhood aggregation (NA), consisting of three key components: membrane potential neighborhood computation, a membrane potential distance measure, and a computationally-efficient backpropagated neighborhood aggregation pipeline. NA avoids calculating the conventionally defined error gradient that does not always exist, and instead gears towards leveraging finite differences within a neighborhood of each neuron's membrane potential. This leads to the so-called aggregated gradient that is more meaningful for spiking neurons.The superiority of the NA algorithm over the prior arts is demonstrated by benchmarking on commonly used datasets. This work provides a general finite-difference based direct SNN training framework, and leaves great flexibility for developing improved methods of neighborhood selection and finite difference aggregation.

References

Bellec, G., Salaj, D., Subramoney, A., Legenstein, R., and Maass, W. Long short-term memory and learning-to-learn in networks of spiking neurons. *Advances in neural information processing systems*, 2018.

Berner, C., Brockman, G., Chan, B., Cheung, V., Dębiak, P., Dennison, C., Farhi, D., Fischer, Q., Hashme, S., Hesse, C., et al. Dota 2 with large scale deep reinforcement learning. *arXiv preprint arXiv:1912.06680*, 2019.

Blouw, P., Choo, X., Hunsberger, E., and Eliasmith, C. Benchmarking keyword spotting efficiency on neuromorphic hardware. In *Proceedings of the 7th Annual Neuro-inspired Computational Elements Workshop*, pp. 1–8, 2019.

Bohte, S. M., Kok, J. N., and La Poutre, H. Error-backpropagation in temporally encoded networks of spiking neurons. *Neurocomputing*, 48(1-4):17–37, 2002.

Brown, T. B., Mann, B., Ryder, N., Subbiah, M., Kaplan, J., Dhariwal, P., Neelakantan, A., Shyam, P., Sastry, G., Askell, A., Agarwal, S., Herbert-Voss, A., Krueger, G., Henighan, T., Child, R., Ramesh, A., Ziegler, D. M., Wu, J., Winter, C., Hesse, C., Chen, M., Sigler, E., Litwin, M., Gray, S., Chess, B., Clark, J., Berner, C., McCandlish, S., Radford, A., Sutskever, I., and Amodei, D. Language models are few-shot learners. 2020.

Davies, M., Srinivasa, N., Lin, T.-H., Chinya, G., Cao, Y., Choday, S. H., Dimou, G., Joshi, P., Imam, N., Jain, S., et al. Loihi: A neuromorphic manycore processor with on-chip learning. *IEEE Micro*, 38(1):82–99, 2018.

Deng, L., Wu, Y., Hu, X., Liang, L., Ding, Y., Li, G., Zhao, G., Li, P., and Xie, Y. Rethinking the performance comparison between snns and anns. *Neural Networks*, 121: 294–307, 2020.

Furber, S. B., Galluppi, F., Temple, S., and Plana, L. A. The spinnaker project. *Proceedings of the IEEE*, 102(5): 652–665, 2014.

Gerstner, W. and Kistler, W. M. *Spiking neuron models: Single neurons, populations, plasticity*. Cambridge university press, 2002.

Huh, D. and Sejnowski, T. J. Gradient descent for spiking neural networks. *Advances in neural information processing systems*, 2017.

Jin, Y., Zhang, W., and Li, P. Hybrid macro/micro level backpropagation for training deep spiking neural networks. *Advances in neural information processing systems*, 31: 7005–7015, 2018.

Kim, J., Kim, K., and Kim, J.-J. Unifying activation- and timing-based learning rules for spiking neural networks. *Advances in Neural Information Processing Systems*, 2020.

Krizhevsky, A., Hinton, G., et al. Learning multiple layers of features from tiny images. 2009.

Krizhevsky, A., Sutskever, I., and Hinton, G. E. Imagenet classification with deep convolutional neural networks. *Communications of the ACM*, 60(6):84–90, 2017.

LeCun, Y. The mnist database of handwritten digits. *http://yann. lecun. com/exdb/mnist/*, 1998.

Merolla, P. A., Arthur, J. V., Alvarez-Icaza, R., Cassidy, A. S., Sawada, J., Akopyan, F., Jackson, B. L., Imam, N., Guo, C., Nakamura, Y., et al. A million spiking-neuron integrated circuit with a scalable communication network and interface. *Science*, 345(6197):668–673, 2014.

Mostafa, H. Supervised learning based on temporal coding in spiking neural networks. *IEEE transactions on neural networks and learning systems*, 29(7):3227–3235, 2017.

Niu, X., Li, B., Li, C., Xiao, R., Sun, H., Deng, H., and Chen, Z. A dual heterogeneous graph attention network to improve long-tail performance for shop search in e-commerce. In *Proceedings of the 26th ACM SIGKDD International Conference on Knowledge Discovery & Data Mining*, pp. 3405–3415, 2020.

Orchard, G., Jayawant, A., Cohen, G. K., and Thakor, N. Converting static image datasets to spiking neuromorphic datasets using saccades. *Frontiers in neuroscience*, 9:437, 2015.

Rossum, M. v. A novel spike distance. *Neural computation*, 13(4):751–763, 2001.

Shrestha, S. B. and Orchard, G. Slayer: Spike layer error reassignment in time. *Advances in Neural Information Processing Systems*, 2018.

Victor, J. D. and Purpura, K. P. Metric-space analysis of spike trains: theory, algorithms and application. *Network: Computation in Neural Systems*, 8(2):127–164, 1997.

Wu, Y., Deng, L., Li, G., Zhu, J., and Shi, L. Spatio-temporal backpropagation for training high-performance spiking neural networks. *Frontiers in neuroscience*, 12: 331, 2018.

Wu, Y., Deng, L., Li, G., Zhu, J., Xie, Y., and Shi, L. Direct training for spiking neural networks: Faster, larger, better. In *Proceedings of the AAAI Conference on Artificial Intelligence*, volume 33, pp. 1311–1318, 2019.

Yang, Y. Temporal surrogate back-propagation for spiking neural networks. *arXiv preprint arXiv:2011.09964*, 2020.

Ye, D., Chen, G., Zhang, W., Chen, S., Yuan, B., Liu, B., Chen, J., Liu, Z., Qiu, F., Yu, H., et al. Towards playing full moba games with deep reinforcement learning. *Advances in Neural Information Processing Systems*, 2020.

Zenke, F. and Ganguli, S. Superspike: Supervised learning in multilayer spiking neural networks. *Neural computation*, 30(6):1514–1541, 2018.

Zhang, W. and Li, P. Spike-train level backpropagation for training deep recurrent spiking neural networks. *Advances in neural information processing systems*, 2019.

Zhang, W. and Li, P. Temporal spike sequence learning via backpropagation for deep spiking neural networks. *Advances in Neural Information Processing Systems*, 33, 2020.